

Altered Myocardial Motion Pattern in Fabry Patients Assessed with CMR-Tagging

Andrea K. Rutz,¹ Christoph F. Juli,² Salome Ryf,¹ Urs Widmer,³ Sebastian Kozerke,¹
Boris P. Eckhardt,² and Peter Boesiger¹

Institute for Biomedical Engineering, University and ETH Zurich, Switzerland;¹ Institute for Clinical Radiology, Cantonal Hospital Winterthur, Switzerland;² Internal Medicine Department, University Hospital Zurich, Switzerland³

ABSTRACT

Progressive left ventricular hypertrophy is the hallmark of cardiac manifestations in patients with Fabry disease. Cardiovascular magnetic resonance with tissue tagging allows detailed assessment of the cardiac motion pattern. The aim was to test the hypothesis that not only Fabry patients with severe left ventricular hypertrophy exhibit changes in myocardial motion, but also Fabry patients with normal left ventricular mass. Magnetic resonance tagging using slice following complementary spatial modulation of magnetization (CSPAMM) combined with harmonic phase analysis (HARP) was applied to measure left ventricular shortening and contraction. Additionally, left ventricular rotation and global left ventricular torsion were examined. Twenty-nine Fabry patients grouped in patients with ($n = 13$) and without ($n = 16$) left ventricular hypertrophy were compared with 29 age and sex matched healthy volunteers. Long axis shortening and circumferential contraction showed reduced peak values with increasing left ventricular mass and were significantly reduced in Fabry patients with left ventricular hypertrophy ($p < 0.001$ and $p < 0.05$, respectively). Torsional deformation and apical rotation were increased both in Fabry patients with left ventricular hypertrophy as well as in patients with normal left ventricular mass ($p < 0.001$ for torsion) compared with controls. Applying the magnetic resonance tagging acquisition and analysis methods, myocardial motion abnormalities could not only be measured in Fabry patients with left ventricular hypertrophy but also in patients without macroscopic cardiac involvement.

INTRODUCTION

Fabry disease (FD) is an X-linked inherited deficiency of the lysosomal enzyme α -galactosidase. This deficiency

leads to progressive intracellular accumulation of glycosphingolipids in various tissues. Left ventricular (LV) hypertrophy (LVH) is the hallmark of cardiac manifestations in affected patients, worsening with age and sometimes leading to death (1).

Before the availability of enzyme replacement therapy (ERT), myocardial involvement of Fabry disease was monitored by ultrasound using functional (ejection fraction, EF) and volumetric (hypertrophy) parameters. Echocardiography based on Doppler imaging has shown changes in regional motion patterns, such as reduced myocardial contraction and relaxation velocities in Fabry patients with LVH (2, 3). Similar regional motion abnormalities were found to a lesser extent in non-hypertrophic hearts of Fabry patients (3). Echocardiographic measurements, however, have several limitations. A poor acoustic window and through-plane motion (up to 2 cm at the basal level in healthy volunteers [4]), due to systolic shortening, can significantly compromise the measured results.

Cardiovascular magnetic resonance (CMR) with myocardial tagging is a powerful method to non-invasively quantify myocardial motion (5). With CMR, image slices can be measured in arbitrary locations and angulations, and the technique

Received 30 January 2007; accepted 12 July 2007.

Keywords: Fabry Disease, Tagging, Hypertrophy, Myocardial Contraction.

The authors are grateful for the continuing support of Philips Medical Systems and the financial support by the Strategic Excellence Program (SEP) of the ETH Zurich. Additionally, this research has been supported by Transkaryotic Therapies (TKT) and the Swiss National Center of Competence in Research on Computer Aided and Image Guided Medical Interventions (NCCR CO-ME) of the Swiss National Science Foundation.

Correspondence to:

Andrea Rutz, MSc
University and ETH Zurich
Institute for Biomedical Engineering
Gloriastrasse 35
CH-8092 Zurich
Switzerland

tel: ++41 44 632 7707; fax: ++41 44 632 1193
email: rutz@biomed.ee.ethz.ch

is independent of acoustical windows. Complementary spatial modulation of magnetization (CSPAMM) (6) combined with harmonic phase analysis (HARP) (7) allow for automated motion tracking of tissue points throughout the cardiac cycle with minimal user interaction. The application of a slice-following technique (8) guarantees reliable measurement of identical anatomical regions during the cardiac cycle without through-plane motion effects. By applying peak-combination HARP (9), a recent extension of HARP, artifacts arising from imperfections, such as patient-induced magnetic field inhomogeneities, can be suppressed resulting in improved reliability and reproducibility of the HARP post-processing. Furthermore, additional deformation parameters, such as LV rotation and torsion, can be assessed with CMR tagging. Previous studies have shown that these parameters are important for the characterization of cardiac motion in patients with LV hypertrophy in hypertensive heart disease (10, 11).

Since volumetric and functional changes occur late in the natural course of Fabry disease and do not change rapidly under ERT, a sensitive imaging modality is needed to capture subtle changes in cardiac motion. CMR imaging with myocardial tagging was therefore thought to be a valuable and feasible alternative imaging method. The purpose of the present study was to prospectively test the hypothesis that CMR imaging can detect abnormal myocardial motion not only in Fabry patients with severe LV hypertrophy but also in patients without macroscopic cardiac involvement, i.e., in patients with a normal LV mass.

METHODS

Study population

Twenty-nine patients with Fabry disease underwent CMR imaging as part of their routine diagnostic work-up. Twenty-nine age and sex matched healthy volunteers underwent the same imaging procedure. Written informed consent from all subjects and institutional review board approval were obtained.

The study population consisting of 29 subjects (17 male, 12 female) with genetically confirmed Fabry disease was grouped as follows: 16 patients with normal LV mass (FD_{normal}) and 13 patients with LV hypertrophy (FD_{LVH}). The cutoff for LVH was defined gender dependently by increased LV mass normalized to body surface area, as described in (12). The mean age of all Fabry patients was 37.6 years with a standard deviation (SD) of 12.8 years. All patients except six females without LVH and two males with LVH received ERT at the time of the measurement. More detailed characteristics of the patient groups are given in Table 1.

A control population of 29 age and sex matched healthy volunteers (17 male, 12 female) was examined for comparison and grouped corresponding to each group of Fabry patients with (Vol_{c_LVH}) and without LVH (Vol_{c_normal}). None of the volunteers showed LVH or had a known history or signs of cardiovascular disease. The mean age of all control subjects was 37.5 with a

Table 1. Characteristics of Fabry Patients

	FD _{normal}	FD _{LVH}
men/women	6/10	11/2
age [years]	32.3 ± 11.6	44.2 ± 11.3
weight [kg]	61.1 ± 10.2	66.8 ± 9.6
heart rate [bpm]	61.8 ± 8.9	61.7 ± 10.0
LV mass [g]	94.1 ± 19.7	180.5 ± 52.5
LV mass/BSA [g/m ²]	55.3 ± 9.6	100.5 ± 24.3
SV [mL]	79.3 ± 16.9	110.9 ± 31.6
EF [%]	63.6 ± 7.7	70.4 ± 7.2
ERT	10	11
ERT duration [yrs]	2.1 ± 0.8	1.9 ± 0.8

For each group of patients, the following characteristics are given: number of measured male and female individuals, age, weight, heart rate, left ventricular (LV) mass, LV mass normalized to body surface area (BSA), LV stroke volume (SV), ejection fraction (EF), the number of subjects that underwent enzyme replacement therapy (ERT) at the time of measurement and duration of ERT in these patients. All values are indicated as mean ± 1 SD.

SD of 12.5 years (32.3 ± 11.1 years for Vol_{c_normal} and 43.9 ± 11.8 years for Vol_{c_LVH}).

Data acquisition

For planning purposes and to determine the timing of mitral valve opening, a four-chamber view was acquired with a steady state free precession (SSFP) sequence (25 cardiac phases and a temporal resolution of about 30 ms depending on the heart rate).

To assess LV mass in patients with Fabry disease, multi-slice short-axis SSFP data-sets covering the entire left ventricle were acquired as described in (12), with 25 heart phases per cardiac cycle.

For the quantification of LV circumferential shortening, rotation and torsion, short-axis CSPAMM images were acquired in all subjects on apical, midventricular and basal cardiac levels. The exact slice level locations were determined by dividing the distance between the level of the mitral annulus and the epicardial contour of the apex into four equal segments on the four-chamber SSFP scan. Three parallel CSPAMM slices were then positioned orthogonally to each of the 3 inner segment borders. In order to compensate for through-plane motion, a slice following technique (8) was applied, and an optimized ramped flip angle approach was used to prevent tag fading during the cardiac cycle (6, 13). Two tagged cine image series with orthogonal one-dimensional stripe patterns and 8 mm tag distance were acquired in one breath-hold on a 1.5 T MRI scanner (Gyrosan Intera, Philips Medical Systems, Best, the Netherlands). The imaging parameters of the EPI sequence were as follows: slice thickness: 8 mm, EPI factor: 11, FOV: 330 × 264 mm², matrix: 128 × 33. Depending on the heart rate, approximately 20 frames were recorded with a temporal resolution of 25–35 ms and a final flip angle of around 20°. For signal reception, a phased array coil consisting of five coil elements (two on the chest, three on the back) was used.

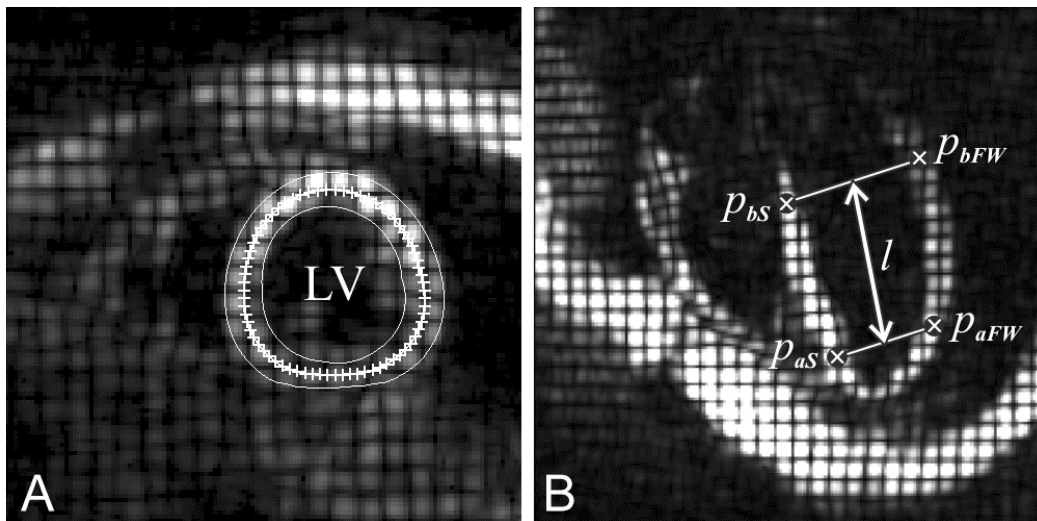


Figure 1. Definition of landmark points for HARP tracking on CSPAMM images of a healthy volunteer: A) LV short-axis image with a midwall contour centered between the semi-automatically identified myocardial borders (thin lines). B) Measurement of LV long-axis shortening on a four-chamber view image. For each of the base and the apex, landmark points on the septum (p_{bS} , p_{aS}) and the free wall (p_{bFW} , p_{aFW}) were identified for tracking. From their actual locations, l was calculated in order to determine LV long-axis shortening.

LV long-axis shortening during the cardiac cycle was assessed in a subset of 20 patients with Fabry disease vs. the same number of age and sex matched healthy volunteers. Six patients exhibited LVH (4 males), and 14 had normal LV mass (5 males). CSPAMM images were acquired in four-chamber view orientation with identical scan parameters as above.

Additionally, late gadolinium enhanced images with inversion time set to null healthy myocardium were acquired 10 min after contrast injection in all patients.

Data analysis

All data were analyzed with HARP (7) using an in-house software tool (TagTrack, GyroTools Ltd., Zurich, Switzerland). To compensate for phase errors due to patient induced magnetic field inhomogeneities and to increase HARP accuracy, peak-combination HARP (9) was applied. Since phase errors additive to both harmonic peaks are eliminated by peak-combination HARP, phase contributions originating from different coil locations are inherently compensated for as well. Hence, peak-combined HARP images of different coil elements could be combined in a straightforward fashion during post-processing to achieve a more homogeneous quality of the HARP images across the field of view. With a tag distance of 8 mm and HARP-filtering, the spatial resolution of the obtained displacement data was approximately $13 \times 13 \text{ mm}^2$ (14).

The endo- and epicardial borders were semi-automatically determined in a time frame without visible artifacts and with good blood-myocardium contrast, i.e., at later heart phases, as described by Ryf et al. (15). A centerline consisting of 72 regularly distributed landmark points was calculated (Fig. 1A). The

centerline was subsequently HARP-tracked through all time frames. Circumferential shortening (CSh in %) at each time frame was defined as the relative length change of the centerline with respect to the original length at end-diastole (first time frame).

The rotation angle of the centerline was calculated for each acquired heart phase by determining the average difference between the actual angles of all points on the centerline and the corresponding original angles at end-diastole. Both the circumferential shortening and the rotation angle were calculated according to the detailed descriptions given by Ryf et al. (16).

Furthermore, the relative global torsion ϕ (in deg/cm) of the left ventricle was determined for each heart phase hp by subtracting the rotation angle φ of the centerline at the basal slice from the rotation angle at the apical slice. The result was then divided by the distance d (in cm) between the two acquired slices for normalization purposes:

$$\phi(hp) = \frac{\varphi_{\text{apex}}(hp) - \varphi_{\text{base}}(hp)}{d}.$$

The maximal diastolic untwisting velocity of the apex and the maximal torsional recoil velocity of the left ventricle during diastole were determined by calculating the temporal derivatives of the rotation angle and the torsion.

For the analysis of LV long-axis shortening (LAS, in %), HARP tracking was applied to landmark points located at the apical and the basal level of the septum (p_{aS} , p_{bS}) and the free wall (p_{aFW} , p_{bFW}) (Fig. 1B). The apical and the basal levels used were identical to the levels at which the tagged short-axis images were acquired. From the locations of the four landmark

Table 2. Maximum LV Deformation Values for Fabry Patients and Volunteers

	FD _{normal}	FD _{LVH}	Vol _{c_normal}	Vol _{c_LVH}
LAS [%]	19.3 ± 1.8	12.5 ± 2.5***	19.8 ± 1.8	18.7 ± 1.1
apical CSh [%]	24.9 ± 2.3	19.9 ± 4.6*	23.5 ± 2.2	22.9 ± 2.0
equatorial CSh [%]	22.9 ± 2.0	19.7 ± 2.5	21.3 ± 2.1	21.5 ± 1.7
basal CSh [%]	21.2 ± 2.0*	18.0 ± 2.6	19.3 ± 1.9	19.6 ± 1.6
apical rot [deg]	12.9 ± 2.6**	13.3 ± 3.0**	9.8 ± 2.2	10.1 ± 3.2
equatorial rot [†] [deg]	5.4 ± 2.0	4.1 ± 1.8	4.3 ± 1.8	5.1 ± 2.7
basal rot [†] [deg]	-0.2 ± 3.0	-1.8 ± 2.3	-0.4 ± 2.6	0.5 ± 2.2
torsion [deg/cm]	3.3 ± 0.6***	3.2 ± 0.8*	2.3 ± 0.5	2.5 ± 0.5

Maximum values of long-axis shortening (LAS), circumferential shortening (CSh), rotation (rot) and torsion are listed for the left ventricle. All values are indicated as mean ± 1 SD.

[†]For the equatorial and the basal cardiac levels, rotation at maximum apical rotation was compared.

* p < 0.05, ** p < 0.01, *** p < 0.001 vs. corresponding group of volunteers.

points, LAS was calculated as the relative length change of l (Fig. 1B) with respect to the length at the end-diastolic time frame:

$$l(hp) = \frac{\sqrt{\left(\frac{x(p_{bS}, hp) + x(p_{bFW}, hp)}{2} - \frac{x(p_{aS}, hp) + x(p_{aFW}, hp)}{2}\right)^2 + \left(\frac{y(p_{bS}, hp) + y(p_{bFW}, hp)}{2} - \frac{y(p_{aS}, hp) + y(p_{aFW}, hp)}{2}\right)^2}}{\left(\frac{y(p_{bS}, hp) + y(p_{bFW}, hp)}{2} - \frac{y(p_{aS}, hp) + y(p_{aFW}, hp)}{2}\right)^2}$$

$$LAS(hp) = \left(1 - \frac{l(hp)}{l(hp=0)}\right) \cdot 100\%.$$

In order to correct for different heart rates, temporal resolution and number of frames, all circumferential shortening, rotation, torsion and LAS curves were resampled and temporally normalized to end-systole (ES). Due to irregular time courses of LV contraction in some of the patients, end-systole was defined relative to the moment of mitral valve opening determined on the SSFP four-chamber images.

Statistics

The extracted myocardial motion parameters were plotted as mean ± SD. Differences in the peak values of the measured motion parameters between each group of patients with Fabry disease (FD_{normal}, FD_{LVH}) and the corresponding group of volunteers (Vol_{c_normal}, Vol_{c_LVH}) were compared with an analysis of variance (ANOVA) followed by Bonferroni post-hoc testing (InStat, 3.01, GraphPad Software Inc., San Diego, California, USA). Rotation values at the basal and the midventricular levels were assessed at peak apical rotation. Additionally, to test motion parameters for dependencies on LV mass normalized to body surface area, linear regressions were calculated. P values < 0.05 were considered statistically significant.

RESULTS

The time interval between the R-wave (ECG) and the opening of the mitral valve (as determined on the SSFP four-chamber

view images) was 420.2 ± 36.5 ms for Fabry patients without LVH and 448.7 ± 30.3 ms for patients with LVH. In the volunteers, values were 455.9 ± 38.6 ms for the group corresponding to patients without LVH (Vol_{c_normal}) and 430.1 ± 49.8 ms for the group corresponding to patients with LVH (Vol_{c_LVH}). By calculating the average moment of peak LV contraction in the volunteers, end-systole was defined as 83% of the time interval between the R-wave of the ECG (end-diastole) and mitral valve opening.

Table 2 lists the maximum deformation parameters for each examined group of patients and volunteers. Due to inaccurate planning of the basal slice in two patients with LVH, the statistical data of the corresponding results (basal circumferential shortening, basal rotation, torsion) are reduced by two subjects. None of the patients except one female with LVH exhibited late gadolinium enhancement. In this patient, the scarred region amounted to only 1.4% of the total LV myocardial volume, and no regional motion abnormalities could be observed in the affected area as compared to regions with healthy tissue.

The time courses of LV long-axis shortening and apical circumferential shortening averaged over each group of patients and volunteers are displayed in Fig. 2 (error bars represent 1 SD in all Figs.). Fabry patients without LVH did not exhibit changes in LV long-axis shortening (Fig. 2A). In contrast, peak long-axis shortening was impaired in the group of Fabry patients with marked LVH with high significance (p < 0.001, Fig. 2A) when compared to healthy volunteers. While the circumferential shortening of the left ventricle showed an increased mean peak value at the basal cardiac level for patients prior to developing LVH (p < 0.05, Fig. 2C), LV contraction was significantly impaired at the apical level (p < 0.05) for patients with LVH compared to the healthy controls (Fig. 2D).

Linear regression analysis of peak LV long-axis shortening in all Fabry patients against LV mass normalized to body surface area resulted in a significant decrease of LV long-axis shortening with increasing LV mass, as shown in Fig. 3 (slope significantly different from zero [p < 0.001] and R² = 0.5885). Furthermore, Fig. 4 shows a significant linear dependency in Fabry patients between decreasing LV circumferential shortening and

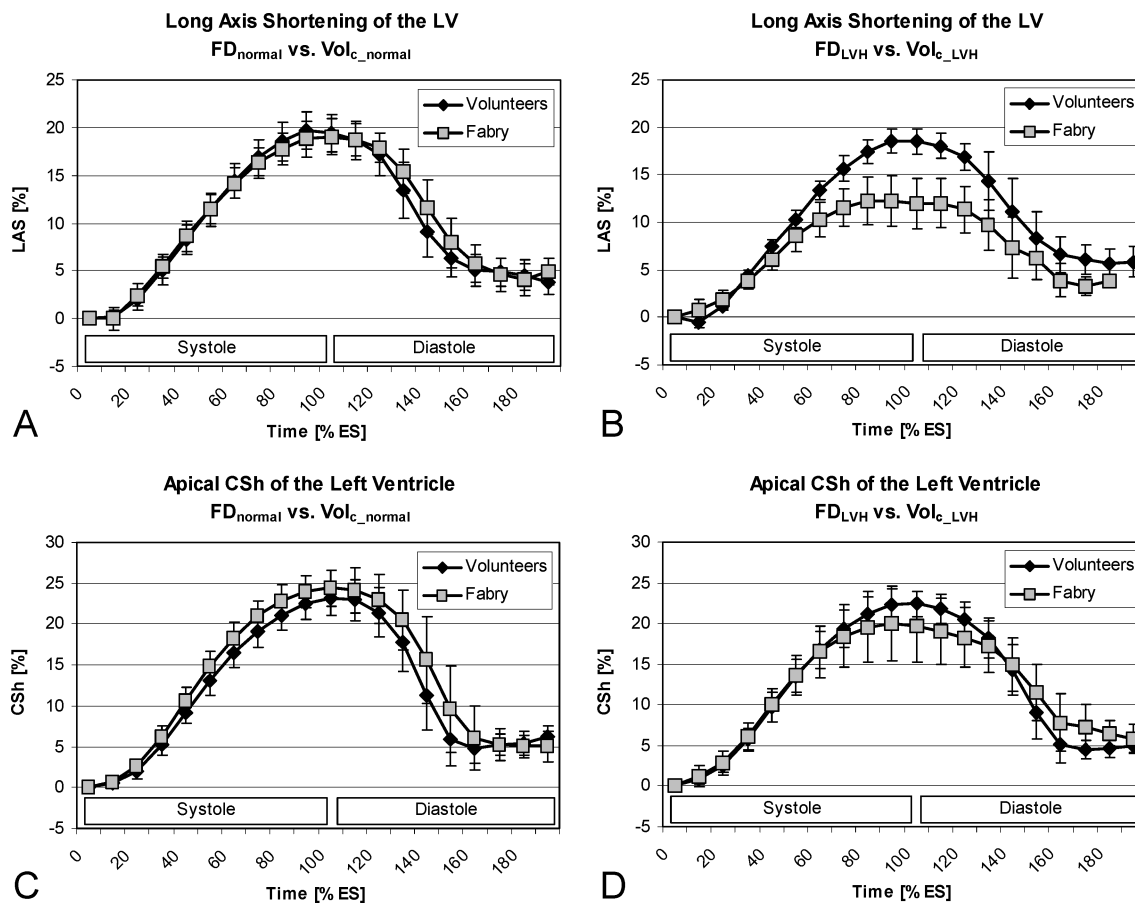


Figure 2. Time curves of LV long-axis shortening (LAS) and circumferential shortening (CSH) over the cardiac cycle normalized to end-systole (ES). Patients with Fabry disease are compared with the corresponding group of volunteers: A, B) LV LAS; C, D) LV apical CSh. While no changes can be observed for patients without LV hypertrophy, significant differences are noticeable around ES for patients with LV hypertrophy. Error bars represent 1 SD in all figures.

increasing LV mass normalized to body surface area (slope different from zero with $p < 0.001$, 0.01 , 0.05 and $R^2 = 0.3372$, 0.2956 , 0.2019 for the apical, equatorial and basal level, respectively).

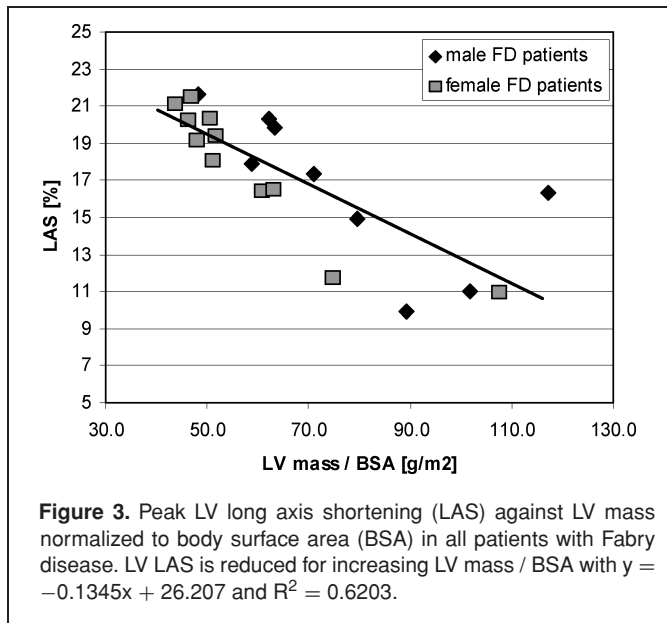
In Fig. 5, apical rotation and LV torsion normalized to ES and averaged over all group subjects are represented over time. Maximum rotation of the left ventricle was significantly increased at the apical level of the Fabry hearts with normal LV mass ($p < 0.001$, Fig. 5A). Similarly, in Fabry patients with LVH, the differences in rotation values at the apex were more pronounced when compared with the controls ($p < 0.001$, Fig. 5B). Altered peak values for the relative global torsion of the left ventricle were found in both groups of patients. Compared to healthy volunteers, highly significant differences were obtained with $p < 0.001$ for patients without LVH and $p < 0.05$ for patients with LVH (Figs. 5C, D). Linear regression resulted in no significant dependencies of rotation or LV torsion on LV mass normalized to body surface area. In Fabry patients with normal LV mass who did not receive ERT, apical rotation was 13.6 ± 1.9 deg, compared to 12.4 ± 2.9 deg in patients without LVH under ERT (non-significant difference). In contrast, LV torsion was signif-

icantly reduced in patients without LVH under ERT compared to patients with normal LV mass who did not receive ERT ($p < 0.05$, 3.0 ± 0.6 deg/cm and 3.7 ± 0.4 deg/cm, respectively).

Table 3 compares the maximum absolute temporal derivatives of the measured rotation and torsion values during diastolic untwisting. Maximum LV rotation velocity at the apex was significantly ($p < 0.01$) increased during diastole in the group of Fabry patients with normal LV mass. Similarly, statistical analysis resulted in a significantly faster LV unwinding velocity during the rapid filling phase for patients without LVH compared to healthy controls ($p < 0.001$). A trend towards higher diastolic untwisting velocities could also be observed for Fabry patients with increased LV mass.

DISCUSSION

The accuracy of echocardiographic techniques such as tissue Doppler imaging or speckle tracking echocardiography is adversely affected by through-plane motion effects, most pronounced at the basal level of the heart (17). This limitation is effectively eliminated with slice-following CSPAMM. The



technique also avoids the problems arising from poor acoustic windows and the difficulties relating to the reproducibility of ultrasound scan plane selection.

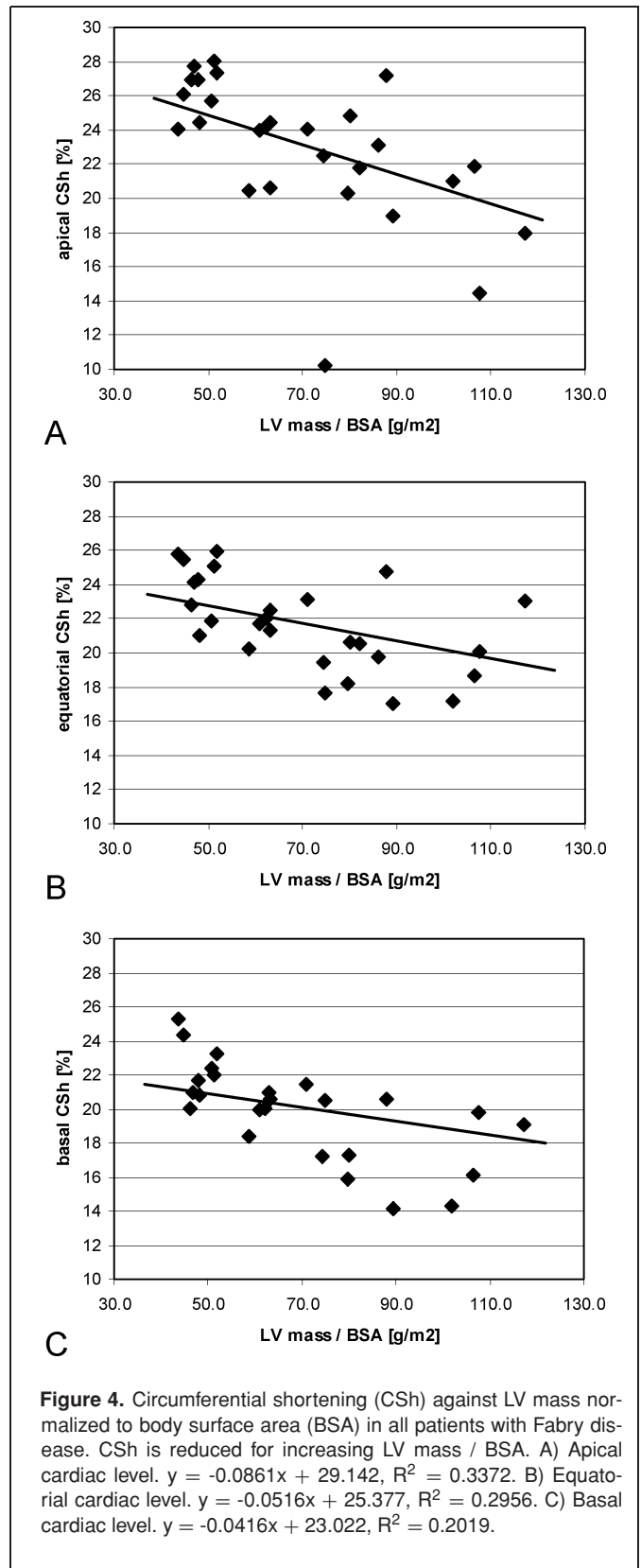
Using CSPAMM and peak-combination HARP, a variety of myocardial deformation parameters can be quantified rapidly and with minimal user interaction. Recently introduced techniques such as peak-combination HARP and semi-automatic definition of landmark points allow for a more accurate and faster assessment of myocardial motion patterns and increase the reproducibility of the examined parameters (9, 15). Since midwall myocardial fibers are oriented mainly in the circumferential direction (18, 19), the shortening of the HARP-tracked centerline approximates well the shortening of the underlying myocardial fibers.

In Fabry patients with LVH, significant functional changes were detected for LV shortening and contraction, which is consistent with results from echocardiographic studies (3, 20). In addition, LV rotation and torsion were examined in this study

Table 3. Maximum LV Untwisting Velocities during Diastole

	FD _{normal}	FD _{LVH}	Vol _{c_normal}	Vol _{c_LVH}
Apical rot [deg/s]	105.8 ± 42.5**	85.8 ± 13.9	75.1 ± 16.3	75.0 ± 21.5
Torsion [deg/cm·s]	28.4 ± 8.4***	24.2 ± 2.2	19.5 ± 5.3	19.1 ± 4.6

Peak diastolic untwisting velocities are listed for the rotation (rot) of the apex and LV torsion. All values are indicated as mean ± 1 SD.
* p < 0.05, ** p < 0.01, *** p < 0.001 vs. corresponding group of controls.



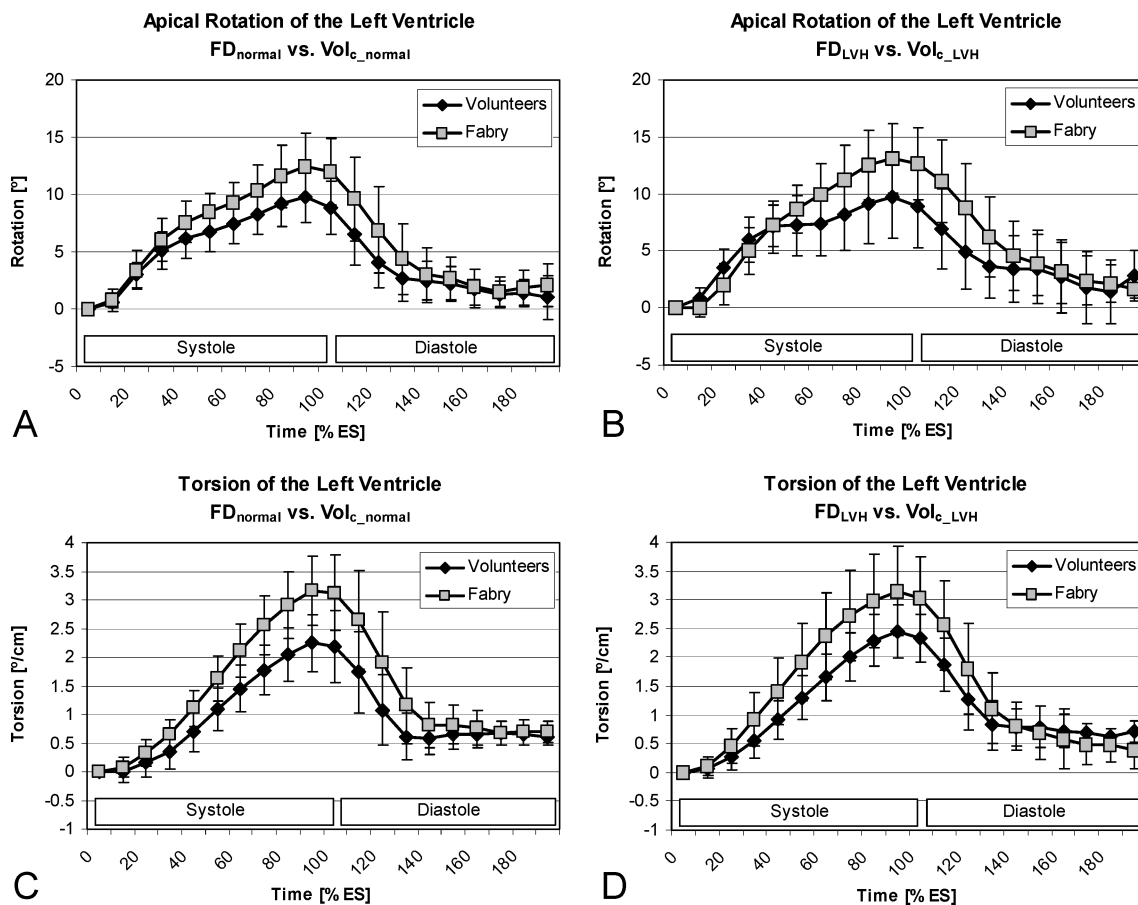


Figure 5. Time curves of LV apical rotation and relative global torsion over the cardiac cycle normalized to end-systole (ES). Patients with Fabry disease are compared with the corresponding group of volunteers: A, B) LV apical rotation; C, D) LV torsion. Significant changes can be noticed not only in Fabry patients with LV hypertrophy but also in patients without LV hypertrophy. Error bars represent 1 SD in all figures.

and significantly altered values were also found for these parameters in the Fabry patients with LVH. The consequence of the increased peak values in rotation and torsion is a faster untwisting of the left ventricle during diastole. Similar results were found in CMR studies where patients with LV pressure overload hypertrophy due to aortic stenosis were examined (11, 21). In these studies, the differences in relative torsion were explained to arise from the complicated LV muscle fiber arrangement combined with an equal sarcomere shortening. Myocardial sarcomeres form a helical structure with varying orientation angle between the endo- and the epicardium, causing substantial torsional deformation in order to maintain transmural homogeneity in sarcomere shortening. Along those lines, Ashikaga et al. concluded in their study of mongrel dog hearts, that the LV mechanics during early relaxation involve substantial deformation of fiber and sheet structures with significant transmural heterogeneity (10). Consequently, global torsional recoil, which is caused by a predominant epicardial stretch along myofibers during isovolumetric relaxation, supports early diastolic filling.

The data of this work suggest that changes of cardiac motion can be detected in patients with Fabry disease before

they develop LVH. Changes in LV rotation and torsion appear to precede the occurrence of morphological changes. The high sensitivity of these parameters in regard to the detection of an altered myocardial function was also reported in previous studies (21–23). Other than in patients with LV hypertrophy due to pressure overload (11), these reduced values of LV rotation and torsion are already visible before development of LVH and seem to be independent of any increase in LV mass. Rearrangement of myocardial fibers and myocardial fibrosis (24, 25) might occur prior to the onset of LVH. This assumption is supported by recent work (26), where the cause for the increase of LV mass in Fabry patients is attributed to a circulating growth-promoting factor rather than to high blood pressure or an accumulation of lysosomal storage bodies in the myocardium. However, values of LV rotation and torsion in Fabry patients without LVH need to be correlated with results from histological examinations to fully confirm this hypothesis. The faster LV untwisting velocities during the rapid filling phase are a direct consequence of the increased values of the rotation and torsion parameters at end-systole.

While rotation parameters seem to be more sensitive for the detection of functional changes in myocardial motion compared to LV contraction and shortening measurements, it has to be considered that rotation values obtained by HARP are less reliable regarding reproducibility compared to circumferential shortening values, as described in (15). This reduced reproducibility of rotation parameters can be explained by their high dependency on the cardiac level between apex and base, meaning that small differences in slice position can alter the measured rotation values significantly. However, this effect is minimized in the torsion values due to the subtraction of the rotation values of two slices and the subsequent normalization on the distance between the acquired slices.

In conclusion, CMR with CSPAMM for myocardial tagging and peak-combination HARP is a sensitive tool to detect alterations of myocardial motion among different groups of patients and controls. The acquired data showed that an increase of LV mass in patients with Fabry disease is accompanied by impaired LV shortening and contraction. By measuring additional cardiac motion parameters such as LV rotation and torsion, early cardiomyopathy in patients with Fabry disease could be detected already before the development of LVH. Further investigation is required to examine early structural changes within the myocardium and the influence of ERT on the assessed motion parameters.

REFERENCES

- Desnick RJ, Ioannou YA, Eng CM. α -Galactosidase A deficiency: Fabry disease. In: Scriver CR, Beaudet AL, Sly WS, Valle D. *The Metabolic and Molecular Bases of Inherited Disease*. 8th Ed. McGraw-Hill, New York, 2001;pp 3733–3774.
- Weidemann F, Breunig F, Beer M, Sandstede J, Turschner O, Voelker W, Ertl G, Knoll A, Wanner C, Strotmann JM. Improvement of cardiac function during enzyme replacement therapy in patients with Fabry disease: a prospective strain rate imaging study. *Circulation* 2003;108:1299–1301.
- Pieroni M, Chimenti C, Ricci R, Sale P, Russo MA, Frustaci A. Early detection of Fabry cardiomyopathy by tissue Doppler imaging. *Circulation* 2003;107:1978–1984.
- Rogers WJ, Jr., Shapiro EP, Weiss JL, Buchalter MB, Rademakers FE, Weisfeldt ML, Zerhouni EA. Quantification of and correction for left ventricular systolic long-axis shortening by magnetic resonance tissue tagging and slice isolation. *Circulation* 1991;84:721–731.
- Axel L, Dougherty L. Heart wall motion: improved method of spatial modulation of magnetization for MR imaging. *Radiology* 1989;172:349–350.
- Fischer SE, McKinnon GC, Maier SE, Boesiger P. Improved myocardial tagging contrast. *Magn Reson Med* 1993;30:191–200.
- Osman NF, Kerwin WS, McVeigh ER, Prince JL. Cardiac motion tracking using CINE harmonic phase (HARP) magnetic resonance imaging. *Magn Reson Med* 1999;42:1048–1060.
- Fischer SE, McKinnon GC, Scheidegger MB, Prins W, Meier D, Boesiger P. True myocardial motion tracking. *Magn Reson Med* 1994;31:401–413.
- Ryf S, Tsao J, Schwitter J, Stuessi A, Boesiger P. Peak-combination HARP: a method to correct for phase errors in HARP. *J Magn Reson Imaging* 2004;20:874–880.
- Ashikaga H, Criscione JC, Omens JH, Covell JW, Ingels NB, Jr. Transmural left ventricular mechanics underlying torsional recoil during relaxation. *Am J Physiol Heart Circ Physiol* 2004;286:H640–647.
- Stuber M, Scheidegger MB, Fischer SE, Nagel E, Steinemann F, Hess OM, Boesiger P. Alterations in the local myocardial motion pattern in patients suffering from pressure overload due to aortic stenosis. *Circulation* 1999;100:361–368.
- Alfakih K, Plein S, Thiele H, Jones T, Ridgway JP, Sivanathan MU. Normal human left and right ventricular dimensions for MRI as assessed by turbo gradient echo and steady-state free precession imaging sequences. *J Magn Reson Imaging* 2003;17:323–329.
- Stuber M, Spiegel MA, Fischer SE, Scheidegger MB, Danias PG, Pedersen EM, Boesiger P. Single breath-hold slice-following CSPAMM myocardial tagging. *Magma* 1999;9:85–91.
- Kuijjer JP, Jansen E, Marcus JT, van Rossum AC, Heethaar RM. Improved harmonic phase myocardial strain maps. *Magn Reson Med* 2001;46:993–999.
- Ryf S, Schwitter J, Spiegel MA, Rutz AK, Luechinger R, Crelier GR, Boesiger P. Accelerated tagging for the assessment of left ventricular myocardial contraction under physical stress. *J Cardiovasc Magn Reson* 2005;7:693–703.
- Ryf S, Rutz AK, Boesiger P, Schwitter J. Is post-systolic shortening a reliable indicator of myocardial viability? An MR tagging and late-enhancement study. *J Cardiovasc Magn Reson* 2006;8:445–451.
- Helle-Valle T, Crosby J, Edvardsen T, Lyseggen E, Amundsen BH, Smith HJ, Rosen BD, Lima JA, Torp H, Ihlen H, Smiseth OA. New noninvasive method for assessment of left ventricular rotation: speckle tracking echocardiography. *Circulation* 2005;112:3149–3156.
- Streeter DD, Jr., Spotnitz HM, Patel DP, Ross J, Jr., Sonnenblick EH. Fiber orientation in the canine left ventricle during diastole and systole. *Circ Res* 1969;24:339–347.
- Reese TG, Weisskoff RM, Smith RN, Rosen BR, Dinsmore RE, Wedeen VJ. Imaging myocardial fiber architecture in vivo with magnetic resonance. *Magn Reson Med* 1995;34:786–791.
- Weidemann F, Breunig F, Beer M, Sandstede J, Stork S, Voelker W, Ertl G, Knoll A, Wanner C, Strotmann JM. The variation of morphological and functional cardiac manifestation in Fabry disease: potential implications for the time course of the disease. *Eur Heart J* 2005;26:1221–1227.
- Nagel E, Stuber M, Burkhard B, Fischer SE, Scheidegger MB, Boesiger P, Hess OM. Cardiac rotation and relaxation in patients with aortic valve stenosis. *Eur Heart J* 2000;21:582–589.
- Delhaas T, Kotte J, van der Toorn A, Snoep G, Prinzen FW, Arts T. Increase in left ventricular torsion-to-shortening ratio in children with valvular aortic stenosis. *Magn Reson Med* 2004;51:135–139.
- Oxenham HC, Young AA, Cowan BR, Gentles TL, Occleshaw CJ, Fonseca CG, Doughty RN, Sharpe N. Age-related changes in myocardial relaxation using three-dimensional tagged magnetic resonance imaging. *J Cardiovasc Magn Reson* 2003;5:421–430.
- Moon JC, Sheppard M, Reed E, Lee P, Elliott PM, Pennell DJ. The histological basis of late gadolinium enhancement cardiovascular magnetic resonance in a patient with Anderson-Fabry disease. *J Cardiovasc Magn Reson* 2006;8:479–482.
- Moon JC, Sachdev B, Elkington AG, McKenna WJ, Mehta A, Pennell DJ, Leed PJ, Elliott PM. Gadolinium enhanced cardiovascular magnetic resonance in Anderson-Fabry disease. Evidence for a disease specific abnormality of the myocardial interstitium. *Eur Heart J* 2003;24:2151–2155.
- Barbey F, Brakch N, Linhart A, Rosenblatt-Velin N, Jeanrenaud X, Qanadli S, Steinmann B, Burnier M, Palecek T, Bultas J, Hayoz D. Cardiac and vascular hypertrophy in Fabry disease: evidence for a new mechanism independent of blood pressure and glycosphingolipid deposition. *Arterioscler Thromb Vasc Biol* 2006;26:839–844.